Fast electrons propagation in high density plasmas obtained by cylindical compression

Contact   **batani@mib.infn.it**

B. Vauzour, F. Dorchies, C. Fourment, S. Hulin, Ph. Nicolaï and J. J. Santos
Université de Bordeaux - CNRS - CEA, Centre Lasers Intenses et Applications (CELIA), Talence, F-33405, France

D. Batani, R. Jafer and L. Volpe
Dipartimento di Fisica, Università di Milano-Bicocca, Italy

M. Koenig, S. D. Baton, E. Brambrink and F. Perez
Laboratoire pour l'Utilisation des Lasers Intenses, Palaiseau, France

M. Galimberti, R. Heathcote, K. Lancaster and C. Spindloe
Central Laser Facility, STFC, Rutherford Appleton Laboratory, HSIC, Didcot, Oxon OX11 0QX, UK

F. N. Beg, S. Chawla and D. P. Higginson
University of California, San Diego, La Jolla, USA

L. Gizzi, P. Koester and L. Labate
ILIL-IPCF, Consiglio Nazionale delle Ricerche, PISA, Italy

A. J. MacKinnon and A. G. MacPhee
Lawrence Livermore National Laboratory, USA

C. Benedetti and A. Sgattoni
Dipartimento di Fisica, Università di Bologna, Italy

J. Pasley
Department of Physics, University of York, YO10 5DD, UK

M. Richetta
Dipartimento di Ingegneria Meccanica, Università di Roma Tor Vergata, Italy

J. J. Honrubia
Universidad Politécnica de Madrid, Spain

W. Nazarov
University of St Andrews, School of Chemistry, St Andrews, UK

Introduction

In the context of the fast ignition scheme in inertial confinement fusion, an energetic electron current, produced by an ultra-intense laser, heats a highly compressed DT plasma core [1]. The fast electrons must transport a few 10 kJ of energy from their source, near critical density, to the high density fuel, after propagation over a few 100 μm of overdense plasma. In order to understand the mechanisms of the electron transport in dense matter some experiments have been successfully carried out in solid targets. However, for those experiments, the reached densities and temperatures are far from those expected in a fast ignition target, namely for the HiPER project [2], and fast electrons propagation will probably have a different behaviour in such conditions. Whilst not yet being able to reproduce the fusion target core density and temperature, it is important to study fast electrons transport and energy deposition in warm and dense plasmas, representative either of the degeneracy of the compressed fuel or of the density and temperature levels near the fast electron source. It is possible to reach such conditions by radially compress cylindrical targets [3]. We have used this geometry in an experiment performed on the Vulcan TAW laser facility at RAL. A first phase (presented in a previous report) consisted in studying the cylindrical target compression to evaluate the targets' core density and temperature radial profiles at different moments of the implosion. A second phase, reported here, was devoted to the study of fast electrons propagation in such compressed targets.

Experiment setup

Four synchronised long laser beams (4×70 J, 1 ns, $\lambda = 0.53$ μm) were used to radially compress
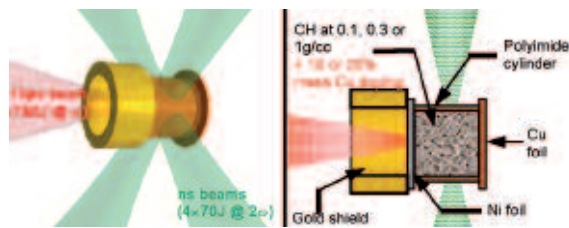
Figure 1. In-principle scheme and target design.

cylindrical targets. A short high intensity laser beam (5×10^{18} W/cm², 10 ps, $\lambda = 1.06$ μm) was focused along the cylinder axis to generate a fast electron current at different times of the compression (see Figure 1). The targets were composed of a 200 μm long, 220 μm diameter and 20 μm thick polyimide cylinder ($\rho_{poly} = 1.1$ g/cc) filled with CH polymerized at three different initial densities ($\rho_0 = 0.1$, 0.3 and 1 g/cc). The cylinders were closed on both sides by 20 μm thick foils, made of Ni at the front side and Cu at the rear side. In order to limit the alteration of the ps beam caused by the low density plasma generated by long pulses, a tube-shaped plastic coated gold shield was stuck onto the Ni foil (see Figure 1). The fast electrons were produced by the interaction of the high intensity laser beam with the Ni foil. To generate electrons at various times during compression, a delay τ was introduced between short (SP) and long pulse (LP) beams with an accuracy of ± 100 ps (due to the jitter).

The fast electrons propagation through the compressed plasma was monitored by the K-shell fluorescence from the Ni and Cu foils. To this purpose, the CH inside the cylinders was doped with 20% mass (only 10% for 1 g/cc targets) of Cu atoms.

Two X-ray Bragg spectrometers were implemented at the rear side of the target to measure the Ni and Cu K-shell fluorescence in the 7.3 - 9.3 keV energy range. The first one was composed by a flat highly oriented pyrolitic graphite (HOPG) crystal with high reflectivity but low spectral resolution (~ 50 eV). The second one consisted of a high spectral resolution (< 5 eV) cylindrical quartz crystal (2d = 2.024 Å, R_c = 100 mm) in a Von-Hamos configuration.

The Cu-K_α emissions (8048 ± 5 eV) from the rear and the transverse sides of the target were collected and imaged with a magnification of ~ 10 onto imaging plates by two spherically bent quartz crystals (2d = 3.082 Å, R_c = 380 mm).

To estimate the hot electrons temperature, a bremsstrahlung hard X-ray spectrometer constituted by a stack of imaging plates and filters, was also used. The analysis of those results is still underway and is not presented in this report.

Experimental results

The K_α and K_β fluorescence yields from the Ni foil on the front side of the cylinder are interpreted as a signature of the fast electron source. The Cu-K_α fluorescence yields emitted either from Cu doped CH core or from the rear side Cu layer, were used as a diagnostic of the fast electrons propagation range. A compilation of the results obtained with the HOPG spectrometer is presented in Figure 2. To account for the small shot-to-shot variations of the fast electrons source, the Cu-K_α yields were adjusted to the Ni-K_β yields for each shot. The Cu-K_α / Ni-K_β ratio is used as a normalized measure of the fraction of the hot (> 8 keV) electrons reaching the rear surface of the target. We clearly observe a decrease against ps/ns delay i.e. against compressed foam density. However we cannot observe a clear dependence on the initial foam density. Results from the Von-Hamos spectrometer and from the rear side Cu K_α imager (not presented here) confirm these trends.

The Figure 3 a), b), c) and d) present images of the Cu K_α fluorescence obtained with the side-on imager for 1 g/cc targets at different times of the compression. In these images we can clearly
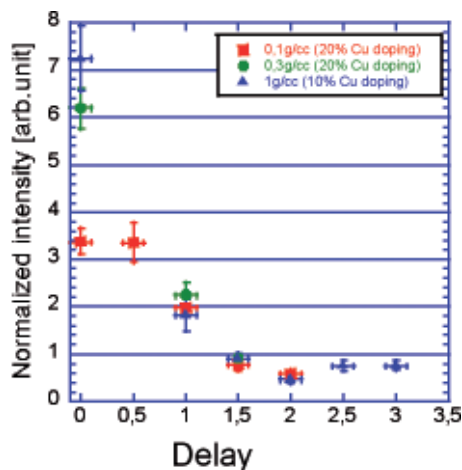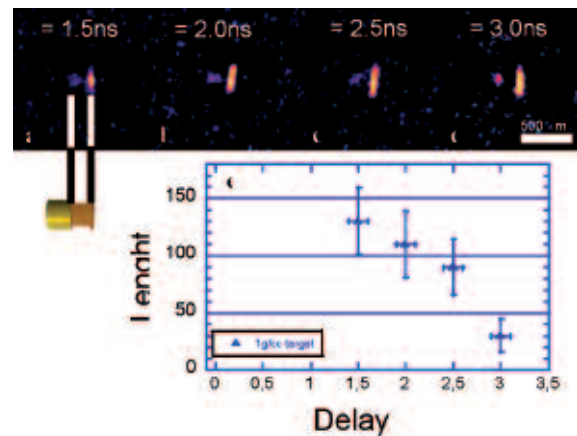
Figure 3 (a, b, c and d). Side-on images of the Cu-K_α emission from the compressed cylinders at different delays for 1 g/cc initial density targets. (e) Length of the targets' core emission against delay (fluorescence emission from the Cu rear foil is not taken into account).

distinguish the emissions from the compressed CH core and from the rear Cu foil (the rear Cu foil is brighter because of its higher Cu atoms density). In Figure 3e the depth of the K_α emission from the target's core is plotted against time. The range decreases with the ps/ns delay: the fast electrons' penetration depth declines from a 130 μm range at the beginning of the compression to 30 μm near the stagnation time τ ≈ 2.3 ns (see report from the first phase of the experiment). This means that the distance covered in the plasma by the rather low energy electrons (< 100 keV, for which the K-shell ionisation cross section is higher) of the incident beam decreases during compression. Together with the spectrometry (Fig. 2) and rear side imaging data, this suggests a rise of the fast electrons energy losses when propagating in plasmas of higher density.

The transverse width of the Cu foil emission at the rear side (the most intense part on the images) is related to the radial extent covered by the fast electron beam at 200 μm depth. These measurements are reported in the Figure 4. Two different behaviours are distinguishable: in the case of low density targets (ρ_0 = 0.1 and 0.3 g/cc) the width decreases against time suggesting the compression contributes to a radial confinement of the fast electron beam. This is opposite to the observed trend in the case of the high density targets (1 g/cc), suggesting a raise of the fast electron beam divergence for rising core density. The investigations in order to explain this difference will be supported by hybrid simulations of the fast electron transport in conjunction to the plasma characterisation obtained in the first phase of the experiment. However, a first explanation could be put forward considering the shell/core density ratio and consequent resistivity ratio. Indeed, for low density targets, the shell is much denser than the core, and this radial structure is conserved during compression. The centripetal resistivity gradient can contribute to a magnetic confinement of the fast electrons along the axis core, as reported in Ref. [4] in a different geometry.

Figure 2. Results from the HOPG spectrometer: comparison of Cu-K_α / Ni-K_β yields ratio against time for different initial target CH core densities.
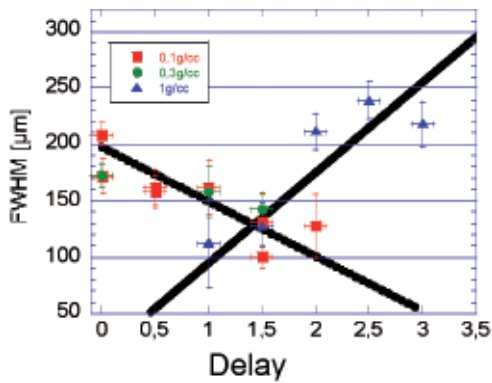
Figure 4. Results from the side-on Cu-K$_\alpha$ imager: width of the emission from the rear Cu foil against time for different initial densities. Dashed and plain lines fit the data from low (ρ_0 = 0.1 and 0.3 g/cc) and high density (ρ_0 = 1 g/cc) targets respectively.

Conclusions

The experiment allowed to observe the fast electrons propagation in high density plasmas obtained by cylindrical compression. For all the tested initial target densities, the fraction of the fast electron population reaching the cylindrical targets rear side decreases during compression. Simulations of the fast electron transport are underway in order to explain the observed fast electron transport features, including energy losses and divergence.

Overall, this experiment was an important testbed for the laser configuration and diagnostics and several challenging experimental points have been clarified.

Acknowledgements

References
1. M. Tabak *et al.*, *Phys. Plasmas* **1**, 1626 (1994).
2. S. Atzeni *et al.*, *Phys. Plasmas* **15**, 056311 (2008).
3. H. Nakamura *et al.*, *Phys. Rev. Lett*. **100**, 165001 (2008).
4. S. Kar *et al.*, *Phys. Rev. Lett*. **102**, 055001 (2009).